

Evasive Maneuvers and Variables Technological Parameters in Orbital Regions Operational

Antonio Delson Conceicao de Jesus¹, Rafael Ribeiro de Sousa² and Ernesto Vieira Neto³

¹ Feira de Santana State University

Received: 11 December 2019 Accepted: 5 January 2020 Published: 15 January 2020

Abstract

In this paper we present results of an analysis on the dynamics of collision between operational vehicles and space debris on a mission in the regions LEO, MEO and GEO. The maneuvers are ideal because in the first instance, we do not consider the existing dissipative forces in these regions. The analysis established technological parameters of the propulsion system of the vehicle that enables the implementation of evasive maneuvers to debris of different sizes (from millimeters to kilometer), speed (0.5 to 20.0 km/s) and positions (3 to 300 km) initials. Furthermore, we assume that these collisional objects are separated by a small distance relative to the distance from the vehicle to earth. The results showed the possibility of collision from a distribution of the initial conditions, including the angles in-plain and out-plain. A policy of compromise between technological parameters and evasive maneuvers of the collisional debris varying size was established, verifying the existence of technological parameters minimum and characteristic for the orbital regions, in favor of schemes to avoid debris from millimeter sizes.

Index terms— space debris; evasive maneuvers, parameters technological

1 Introduction

ince the beginning of the space era, the space environment around Earth became a junk yard full of debris related with space missions. Debris were generated due to explosions (deliberated or not), launch vehicle upper stages, inoperative satellites and even tools and small objects. The millimetre and submillimetre source of debris are propellant residuals, fragmentation processes and ink fillets detached from spacecrafts surface. In 2004 about 40% of debris were generated by explosions and collision involving launch vehicle upper stage or spacecraft in orbit (Bendisich et al., 2004).

The satellite Sputnik 1 launched in 1957 became the first space debris produced by men. 4 years later this launch, the space around the earth had become populated with 300 debris resulted by the explosion of the American Transist-4-A rocket, an explosion which happened 2 hours after reaching orbit. Today, after over 4,900 launches, the space activities produced about 240 further explosions which form the main source of production of space debris (ESA, 2013). With the space race, even with mitigation measures and the natural atmospheric drag in the objects in LEO the distribution of objects in the operating regions increased.

The vehicle propulsion system is responsible for 45.7% of the fragmentation that occur mainly due to catastrophic damage during orbit insertion or others manoeuvres, also there is factors related with failure of the active control system. The growth rate of fragmentation increased since 1970 achieving 5 fragmentation per year (Johnson et al., 2004). Collisions with debris larger than 10 cm are still considered catastrophic and consequently come up a cascade process of other collisions. This type of collision cascade process produces a critical density in long time, and without reduction perspectives, unless the amount of large objects is reduced.

In view of the great need of space missions some control techniques must be adopted to avoid the growth of debris in the operating regions ??Kessler and CourPalais, 1978;Kessler, 1991). Simulations indicate that in a

44 few decades debris from collision fragments will dominate the Earth space in attitudes between 800-1400 km at
 45 least (ESA, 2013). It is clear that the damage to space missions are large, even for smaller debris, since they may
 46 disable or burst operational vehicles and can make infeasible a space mission.

47 The distribution of space debris in LEO, MEO and GEO altitudes causes concerns about the safety of space
 48 activities operations in these regions. The size and altitude of debris are crucial in observing and tracking by
 49 radars. Depending on the accuracy and ability of the radar, smaller debris can be catalogued in higher altitudes.
 50 Optical instruments and radar are able to track and catalogue objects of sizes between 5 and 10 cm in LEO
 51 and sizes between 0.3 and 1 m in GEO (ESA, 2013). This indicates that the latter region can be populated
 52 by smaller and potentially destructive objects not catalogued. In fact, more than 99% of the mass and area of
 53 the population in orbit actually are debris which potentially capable of producing catastrophic rupture (Kessler,
 54 1991).

55 In MEO region orbits the navigation constellations (GPS, GLONASS, etc.) and about 16,000 debris with
 56 diameters larger than 1 cm are predicted to cross orbits in this region. Most of them have non-zero eccentricities,
 57 causing them to reach altitudes of GPS in its apogee. The energy produced in a collision is about 104 J which
 58 could cause severe damage to the spacecraft (Klinkrad, 2006; Rossi, 2005; Rossi and Valsecchi, 2006; Smirnov,
 59 2001). The orbital perturbations in GEO region, different from the atmospheric drag in LEO, does not reduce
 60 the amount of debris (Milani et al., 1987). Since the launch of Syncom-3 in 1964, more than 800 satellites and
 61 rocket stages were placed in this region. The growth rate GEO debris without removal, increases 30 debris per
 62 year (Valk et al., 2009).

63 It is clear that security measures must be taken and evasive manoeuvres must be planned to prevent accidents
 64 among spatial objects. The collisions between operational vehicles with space debris became a reality, although
 65 in the point of statistical view they are rare. In most cases, on average ten risk alarms are generated per year, and
 66 fewer avoidance maneuver are implemented by year (ESA, 2009). But these estimates depend on a combination
 67 of many factors and specialized computer codes.

68 Beyond that there is a lot of uncertainties such as debris related with non-commercial missions, that is,
 69 upper stages and debris linked to certain classes of American secret missions and, more recently, a couple of
 70 Japanese reconnaissance spacecraft, which are not included in the catalogue version available (maintained by
 71 the Space Control Center, operated by the Air Force Space American Command) to commercial and foreign
 72 entities (Godwin, 2003). This account for approximately 4% of the catalogued objects. And there are other
 73 uncertainties that affect the missions in LEO, for example, modelling the uncontrolled satellites trajectory by re-
 74 entry, distortions in the observation of debris that occur in long time observation, the difficulty in predicting solar
 75 and geomagnetic activities which depends on the atmospheric density (Rossi et al., 1998; Anselmo and Trumpy,
 76 1986).

77 This paper studies evasive manoeuvres in operating regions to establish technological parameters that are
 78 efficient to implement. This is a first model without dissipative forces in all regions.

79 Our study does not include dissipative forces, as it aims to establish optimal conditions for the evasive
 80 maneuvers of a vehicle in front of the possibility of collision with space debris. Moreover, the study is restricted
 81 to collisional bodies whose relative distance between them is smaller than the spacecraft to the Earth.

82 2 II.

83 3 The Mathematical Model

84 Our approach is based on the study of the relative movement between a vehicle and a space debris. The reference
 85 system in Figure ?? is fixed on the vehicle. We measure the positions and relative speeds w.r.t. this system, such
 86 that all technical control evasive maneuver is performed from it. The dynamics between these objects not consider
 87 active dissipative forces, only the Earth's gravitational force on the vehicle and the debris and the propulsive
 88 force of the vehicle.

89 We consider that the relative distance between objects is very small compared to the distance from the vehicle
 90 to the center of the Earth, that is, ($r \ll R$). In this condition, the resultant force of gravitational term can be
 91 expanded and analytic solution may be found with significant accuracy (Clohessy-Witshire, 1960). The thrust
 92 adopted in our model is proportional to the rate of exhaustion of the propellant vehicle system and, through it,
 93 the movement can be controlled. The equations for the Cartesian components of the relative acceleration are:

$$94 \ddot{x} - 2\dot{y} = -\frac{\mu}{r^3}x + \dot{w}_x \ln(M(t)) \quad \ddot{y} + 2\dot{x} = -\frac{\mu}{r^3}y + \dot{w}_y \ln(M(t))$$

95 Figure ??: Reference frame for a vehicle around Earth and for a space debris. The frame with capital letters
 96 is positioned in the Earth center.

$$97 \mathbf{r} = (x, y, z)$$

98 These Equations model the relative dynamics between operating vehicle and space debris. For each orbital
 99 region (LEO, MEO, GEO) the vehicle orbits side of these Equations are the components of the nongravitational
 100 acceleration, in which case the components of the acceleration of propulsion. For this dynamics, we adopt
 101 exponential change in mass of the vehicle in time, such that,

102 With m_0 as the initial propellant mass and P is the power factor of the engine. The total mass of the satellite
 103 is dependent of the mass of the propellant:

$$104 m = m_0 - \frac{P}{c} t$$

105 With M_o is the net mass of the satellite disregarding the propellant. $Y X Z x y z$ Earth Spacecraft Debris $r R$
106 $i j k J K ? ? I z + w 2 z = ?v e z d dt \ln(M(t)) m(t) = m_o e^{??t} M(t) = M_o + m(t) w = w k.$

107 4 around the Earth with circular velocity, The

108 We write the mass factor as (??)

109 And then we have (7) The technological parameters identified for this dynamic are:

110 1. Components of the gas exhaust velocity 2. The power factor of the engine $? > 0$ and; 3. And the mass
111 factor (), that is, the mass ratio between the spacecraft mass (M_o) and the initial propellant mass (m_o);

112 The components of the propulsion force are,

113 These Equations show that the evasive maneuver can be controlled by the power factor, maintaining the
114 circular or quasi-circular orbit. We found that for circular orbits in LEO, the value of optimal power factor is
115 10-6 (Jesus et al, 2012). This factor should be reduced to that circular orbits nearly circular or are kept in MEO
116 and GEO, as we shall see. In the Appendix, we show the evolution of the eccentricities of the orbits of these
117 operating regions for our model.

118 5 III.

119 6 Evasive Maneuvers Collision Conditions

120 The necessary condition for the collision between two space objects (operational vehicle and space debris) is its
121 final position relative to cancel an instant t_c , ie, (11) This condition must be satisfied concerning the dynamics
122 through a set of initial conditions that includes the components of velocity and position on the objects. The
123 initial relative position is calculated by scanning the spherical angles (in-plain, , and out-plain, , distributed in
124 the region of space where the collisional objects. The relative initial velocity can be found as a function of time
125 through the homogeneous solution of Equations (??) to (3) to $F_x = F_y = F_z = 0$. We call this set, including
126 the t_c , set of initial conditions collision course (CICC). The CICC elements constitute the collision possibilities in
127 the dynamics on these objects, subject only to gravitational force. It does not determine the collision probability,
128 because the equations of speeds are deterministic and not probabilistic. It admits the collision possibilities in the
129 relative dynamic. Thus, the set (CICC) is obtained by the distribution possibilities in the collision time, mapped
130 by a function of the type, (12) Each pair (

131) provides a possibility of collision between objects. We found the inhomogeneous solution of the Equations
132 (1) (3), whose Cartesian coordinates are:(13) (14) (15)

133 These are the Cartesian components of the final relative position of the objects subject to gravitational and
134 propulsion forces. This vector determines the separation of the objects at each instant. In t_c , determines whether
135 a collision has occurred. All coefficients of these equations depend on the initial conditions and the technical
136 parameters that can generally be written as Therefore, the condition (5) can be controlled from the set of
137 these coefficients through technological parameters suitable for the implementation of evasive maneuvers. These
138 maneuvers are possible every time the final separation between the objects is comparable to the dimensions of
139 them. In this paper, we consider the collisional objects as known-radius spheres.

140 7 a) Implementation and Simulation

141 An operating vehicle in collision with space debris must implement an evasive maneuver to avoid it. The radar
142 installed at the base on Earth or on the vehicle will provide information about the initial relatives position and
143 velocity, and the collision time, t_c . The satellite onboard computer will perform calculations on the possibility of
144 collision and also indicate the coordinates that allow the escape of the collision. In this work, we simulate these
145 conditions, setting the time of collision? = $M_o m_o M(t) = m_o (? + e^{??t}) v_{ex}, v_{ey}, v_{ez}$ (; ? $F_x = ?v$
146 $ex m_o e^{??t} F_y = ?v_{ey} m_o e^{??t} F_z = ?v_{ez} m_o e^{??t} x(t) = 0, y(t) = 0, z(t) = 0 ? r(t) = 0 (r_o, ?o) = [r$
147 $o (? o, ? o), ?o (? o, ? o)] x(t) = 2A \sin(nt) ? 2B \cos(nt) + Et + ? n=1 F_n e^{?n?t} + G y(t) = A \cos(nt) +$
148 $B \sin(nt) ? ? n=1 C_n e^{?n?t} + D z(t) = H \cos(nt) + I \sin(nt) ? ? n=1 J_n e^{?n?t} r_o, ?o L = L(r_o, v_o, v_e$
149 $, ?, ?, n). ? ? Global Journal of Researches in Engineering () Volume Xx X Issue I V ersion I D$

150 and getting the initial conditions in favorable velocities and positions to the collision. Hence, we simulate the
151 dynamics described in Equations (??) to (9) to implement the evasive maneuver.

152 Our numerical simulations of evasive maneuvers followed the following general steps: 1. Chose the orbital
153 region (LEO, MEO, GEO) where collisional objects are and calculate the angular velocity that characterizes; 2.
154 Use the solutions of the homogeneous equations of relative dynamics to calculate the initial relative velocity that
155 allow collisions; 3. Set the collision time and the relative initial distance, r_o , between collisional objects and
156 found angles (), consistent with collisions between objects; 4. Calculate the components of the initial relative
157 position from their values; 5. Select a pair of initial conditions of the CICC set, Equation (??), and t_c ; 6.
158 Chose specific technological parameters for the orbital region; 7. Implement the evasive maneuver the spacecraft,
159 operating the propulsion system, numerically simulating the Equations (??) -(??); 8. Obtain the final value of
160 the relative position between objects, testing the collision condition (5).

161 With these steps we intend to model approximately the realistic conditions of an evasive maneuver on the
162 possibility of a collision. To scan the entire sphere of radius with pairs of angles (),is performed to select those

163 that enable collision. Technological parameters are extracted from the catalog-curves produced in this paper,
 164 consistent with the limits for circular or nearcircular orbits. They characterize the propulsion system of the
 165 vehicle and are used to control their escape from the collision.

166 8 IV.

167 9 Numerical Simulation -Results

168 The numerical simulation of evasive maneuvers should take into account information on the initial conditions, the
 169 time of collision and the characteristics of the propulsion system, represented by the technological parameters.
 170 The collision time should be small compared to the orbital period and sufficient for the evasive maneuver is
 171 implemented. Each element of the set CICC is a possibility of collision. The choice of this element is not
 172 arbitrary, why should characterize a real collision in orbital regions. For the numerical simulations, we chose
 173 the initial relative velocities equal to (7,76 km/s, 4,25 km/s, 1,01 km/s) in LEO, MEO and GEO, respectively,
 174 non-planar maneuvers which they are typical in these regions. We investigated the possibility of collision in a
 175 higher range of these velocities, that is, [1,0 -20,0 km/s].

176 The evasive maneuver is characterized by technological parameters (α , β), with which you can control these maneuvers front of an imminent collision. Equation (1) is valid for
 177 any time. The typical technological information space missions can restrict the solutions to a finite set. The
 178 observations of radar confirm average values of initial relative velocities specific to each operating region and
 179 also the minimum time required to perform the operations for evasive maneuvers. Thus, the simulations will be
 180 carried out in finite time and collision possibilities will also be finite, although in large numbers.

181 In this section we show the results of numerical simulations of the relative dynamics between two collisional
 182 objects (vehicle and space debris).

183 The results show: 1) the distribution of collisions in relative initial velocities ranges; 2) a parametric analysis
 184 of evasive maneuvers, characterizing the efficiency of the propulsion system that implements them. In the
 185 distribution of collisions we call collision possibilities. In implementing the evasive maneuver only use one of
 186 them. Figure 1 shows a reference system centered on the space vehicle. In its origin it focuses a sphere of radius
 187 equal to the relative distance between the vehicle and the space debris. Thus, our simulations vary these distances
 188 between 3 and 500 km, with initial relative velocities between 0 and 20 km/s. Knowing the collision possibilities
 189 in their collision time, we conducted a systematic study of technological parameters that are appropriate for
 190 the implementation of various evasive maneuvers. From there, curvescatalogue are generated, considering the
 191 variation of these parameters over time and size of collisional debris. For each operating region (LEO, MEO and
 192 GEO) choose an element of CICC to implement the evasive maneuvers in the region. In this work, we simulated
 193 various evasive maneuvers, taking into account debris and space vehicles of different dimensions. The evasive
 194 maneuvers will be confirmed based on the final values of the relative positions, comparing them to the sizes of
 195 the space objects.

197 10 a) Possibility of Collisions

198 The possibilities of collision between the space objects (vehicle and satellite) are high, considering a time interval
 199 of 10 6 s. Figure 2 below shows the distribution of collisions depending on the initial relative velocities interval
 200 between objects for the operating regions. For discussion purposes, we divide the range of relative initial velocities,
 201 as follows: 1) low velocitiesbetween 0.0 and 4.0 km/s; 2) medium velocitiesbetween 4.0 and 7.5 km/s; 3) high
 202 velocities -between 7.5 and 10.0 km/s, and; 4) high velocities -between 11.0 and 20.0 km/s.

203 In Figure 2, we note that for any operating region there is little chance of collision for high and very high initial
 204 velocities, if the objects move away initially 3 km. This result is consistent with the expected, since the velocities
 205 decrease with increasing altitude. Moreover, in The same is true for MEO regarding GEO. Obviously, the effect
 206 of the Earth gravitational field, favors the approach of objects in LEO by increasing the collision possibilities.
 207 For the range of initial velocities nulls or nearly nulls, the collision possibilities are virtually the same for any
 208 operating region. Figures 3, 4 and 5 show the results of simulations for other initial relative positions between
 209 the space objects to collision time equal to 10 5 s. This collision time is compatible with orbital periods in MEO
 210 and GEO. For LEO it would be 10 3 s. These results generalize those for $r_0 = 3$ km. That is, the collision
 211 possibilities for high and very high velocities are small to any initial relative position. Proportionally, these
 212 collisions occur, possibly in LEO more than MEO, and MEO more than GEO. For medium velocities, there is
 213 greater possibility of collision if the objects are initially farther away and at higher altitudes. Thus, we say that a
 214 greater risk scenario is established for imminent collision in any relative initial velocity, especially in LEO, MEO
 215 and GEO followed. Moreover, our model does not include dissipative forces occurring in these regions. These
 216 forces interfere with the distribution of physical initial conditions that enable collisions, sometimes favoring them,
 217 sometimes reducing them. Our simulations did not include these forces, and thus our results are an ideal initial
 218 test, establishing physical and technological conditions for complete dynamics with dissipative forces.

11 b) Evasive Maneuvers In Meo And Geo

Knowing the dimensions of the collisional objects, our model determines if the evasive maneuver is sufficient to avoid collision between them. The technological parameters are used to evaluate the feasibility of evasive maneuvers for the set of initial conditions favorable to the collision, the collision time interval. For this study the technological parameters, simulated evasive maneuvers between objects initially separate to 3km, with angles $\theta = 68$ and $\phi = 23$ degrees in MEO and GEO regions. The equivalent study for LEO was held earlier paper (Jesus et al., 2011). The red and pink curves, Figure 6, represent the course of a collision (homogeneous solution of Equations 1, 2 and 3) between the objects in the initial conditions for the MEO and GEO regions, respectively. Curves in blue and green represent their evasive maneuvers, whose initial relative velocities are typical of these regions (4.15 km/s -MEO and 1.01 km/s -GEO). These curves characterize the dynamics with propulsion to escape collision with space debris. They inform the final relative position between collisional objects at each time, obtained by the performance of operational vehicle propulsion thrusters. We note that collisional objects initially separated to 3km escape of the collision at different times and in different operating regions. Moreover, their final relative distances are different, which can characterize different sizes of debris. We note that the curves with propulsion characterize success of evasive maneuvers, as the final relative positions are not zero. This success is in large collision time, such that the continuous propulsion can overcome the gravitational effects on the objects, setting their final relative position and avoiding the collision between them. In all cases with propulsion, the collision is easily avoided in hundreds of kilometers of separation between the objects to these maneuvers under these initial conditions. The maneuver MEO escapes closer to the collision in relation to maneuver in GEO. This fact is associated with the typical initial relative velocities and also the period orbits in these regions. The qualitative behavior shown is general, although the results are specific to these regions with the given initial conditions. Thus, we say that given the initial conditions favorable to the collision, the objects develop a relative dynamics to propulsion, such that as time passes, they leave the collision course, swaying their positions around it to fully escape, featuring the evasive maneuver. These initial conditions are overcome by the performance of the propulsion system. Therefore, the technological parameters of it were efficient in the implementation of the evasive maneuver. Technological parameters are effectively crucial in the implementation of evasive maneuvers. They are related to the propulsion system of the space-craft and the correct choice of these parameters will allow efficient evasive maneuvers. The parameter characterizes the frequency with which the fuel is consumed in time, such that the higher it is, more fuel will be spent on the evasive maneuver. Figures 7 and 8, below, are catalog curves which show the behavior of this factor as a function of collision time and the size of the debris in MEO and GEO, respectively. The results show that small power factors favor evasive maneuvers on a collision course with small debris. Conversely, evasive maneuvers to larger debris will require major power factors. This phenomenon occurs in both operating regions, MEO and GEO. It should be noted, however, that the increase of this factor in continuously burning regime can remove the operating object of their nominal circular orbit. In this model we chose power factor operation MEO and GEO equal to 10 -10 (see Appendix), which ensures the permanency of the operating object in a circular or nearly circular orbits. Moreover, very small power factors prevent the implementation of the evasive maneuver, since the propulsion force is virtually zero. But observing such limits, evasive maneuvers can be performed efficiently to escape collisions with debris of various sizes, depending on the time of collision and the propulsion system characterized by the parameter. We say that the high power factor would favor evasive maneuvers with less risks of collision with cloud debris of any sizes. Another technological parameter that we consider is the mass factor. This quantity measures how much the vehicle mass is greater than the initial mass of the fuel it carries. Figure 9 shows the relationship between this factor to the size of the debris which evasive maneuvers escape into GEO, and the exhaust velocity. The power factor used here is equal to 10¹⁴.

In this Figure we observe that evasive maneuvers with small mass factors are more efficient to escape debris increasing relatively. Higher exhaust velocities are favorable to these maneuvers. To escape of smaller debris, lower exhaust velocities are preferable. However, large mass factors are favorable to the evasive maneuvers against collisions with smaller debris and this is independent, practically, the increasing values or not the exhaust velocities.

The results obtained here for MEO and GEO are equivalent to those found by Jesus et al. (2012) to LEO. Figure 10 below shows the risk curve in LEO, MEO and GEO, under the action of gravity forces and propulsion. They are ideal curves because it does not consider the dissipative forces occurring in these regions. In this curve the dimensions of the debris are distributed as a function of collision time, of altitude and of the vehicle exhaust velocities. We note that the qualitative behavior of the curves remains for any altitude of collisional objects and the quantitative results are a function of exhaust velocity.

We note that with higher exhaust velocities will be possible to escape from collisions with large debris. This means that more powerful propulsion systems are less efficient and less economic for evasive maneuvers in small sizes debris environments. In addition, we observed that the risk of colliding with large sized debris increases with low velocities. This risk is reduced by increasing the exhaust velocities. Therefore, it is preferable and more economical to use small exhaust velocity, since the power of the propulsion system must be preserved for escape maneuvers against collisions with very large sizes of debris. Hence, the need for a propulsion system capable of controlling the magnitude of velocity in non-uniform size distribution of debris environment.

12 d) The Risk Curve how to use it

281
282
283
284
285
286
287
288
289
290
291
292
293
294
295
296
297
298
299

The risk curve, shown in Figure ??1, provides information that can be used in decision-making on a space mission to avoid collisions with space debris. To use this curve should be chosen initially, one octant. In this curve, we choose the angles in-plane and out-plane within the range 68 to 79 degrees and 6 and 39 degrees, respectively. Our results showed that the qualitative behavior displayed in this curve is general for all octants, where are located the collisional objects. There is a relationship between the dimensions of collisional debris with the collision time for every operating region. The exhaust velocity is the coefficient between them. It is essential in the implementation of evasive maneuvers, since it is related to engine power. The use of the risk curve in space missions must follow an algorithm of operations that allow to perform an evasive maneuver. If the propulsion system for variable velocity, so the operating system of the vehicle will have the freedom to make decisions to escape from any debris, based on the information on the collision time. The radar informs the coordinates of the debris and the collision time. The vehicle would be in a specific altitude, for which there is a specific curve as a function of Global Journal of Researches in Engineering () Volume Xx X Issue I V ersion I D exhaust velocity. Thus, based on the collision time and the vehicle altitude the operating system know whether or not escape the debris, depending on its size. The onboard computer will calculate the escape trajectory and the curve will inform if one can escape the specific size debris and this will depend on the velocity that the propellant system is able to implement. If the thruster system is not able to vary the exhaust speed, there will only be a range of sizes of debris it can escape. This range is as large as is the variation of the exhaust velocity values.

V.

13 Conclusion

300
301
302
303
304
305
306
307
308
309
310

Our results showed that the relative dynamics between a vehicle and space debris is rich in collision possibilities in LEO, MEO and GEO. Thus, we say that a greater risk scenario is established for imminent collision in any relative initial velocity, especially in LEO, MEO and GEO followed. Our simulations did not include dissipative forces, and thus are an ideal initial test. The continuous propulsion can be used to avoid collisions with space debris, provided that suitable technological parameters. These parameters can control the evasive maneuvers depending on the size of the debris and collision time. If the vehicle has short time to escape, the evasive maneuver occurs if in imminent collisions with small debris. In this case, small exhaust velocities are preferable. We found a risk curve for orbital maneuvers. This curve informs that a system propulsion with variable exhaust velocities is preferred for the evasive maneuvers. These maneuvers would be more economical and efficient to avoid the collisions with any debris.

¹ ² ³

¹© 2020 Global Journals

²© 2020 Global Journals Evasive Maneuvers and Variables Technological Parameters in Orbital Regions Operational

³D © 2020 Global Journals Evasive Maneuvers and Variables Technological Parameters in Orbital Regions Operational

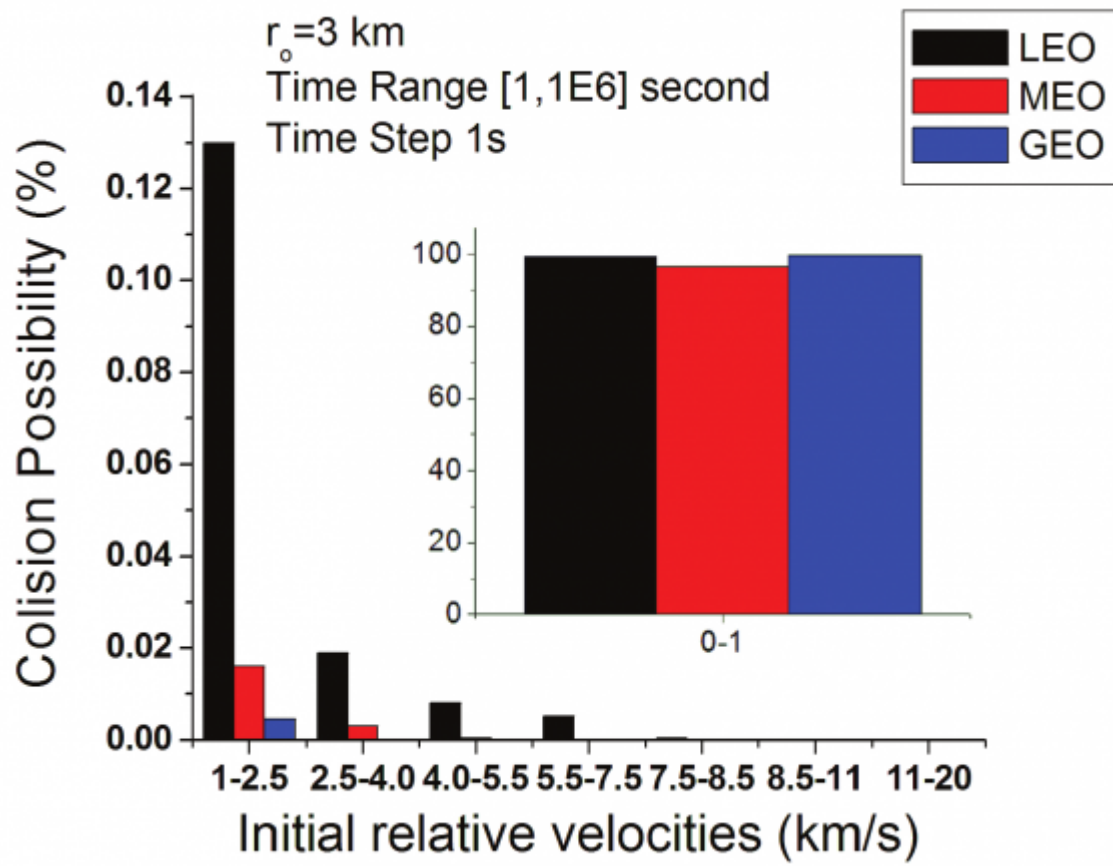
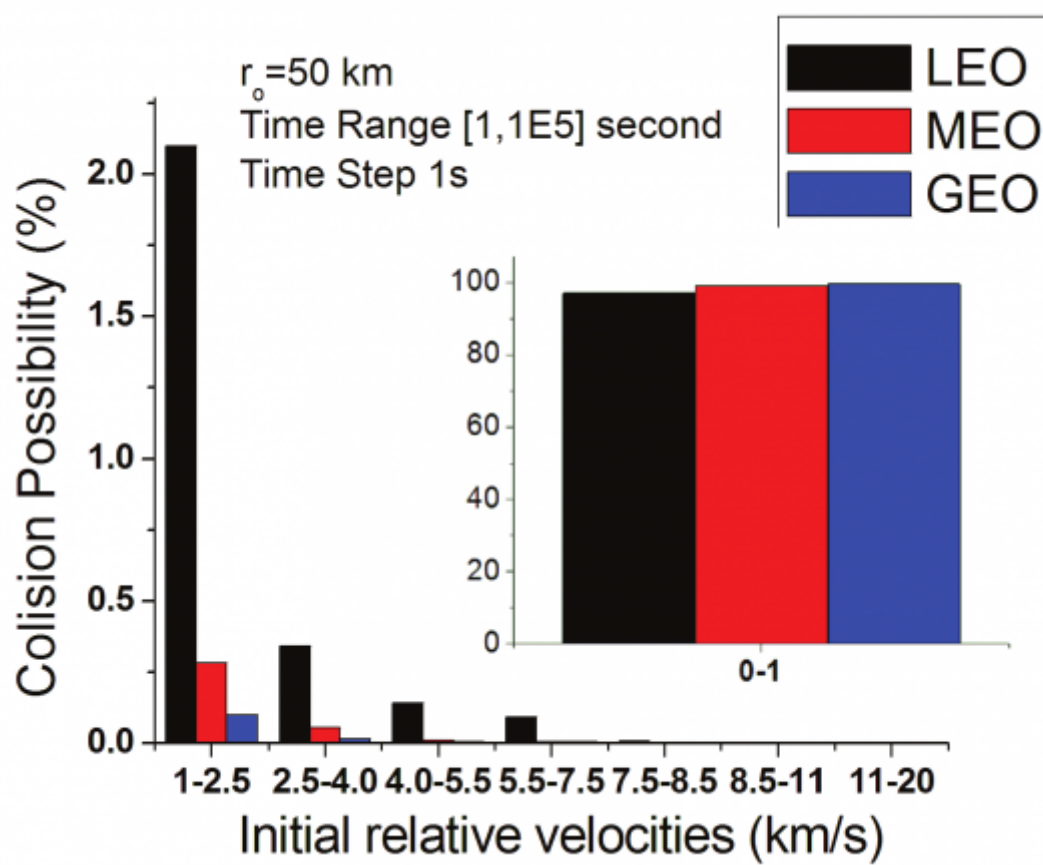
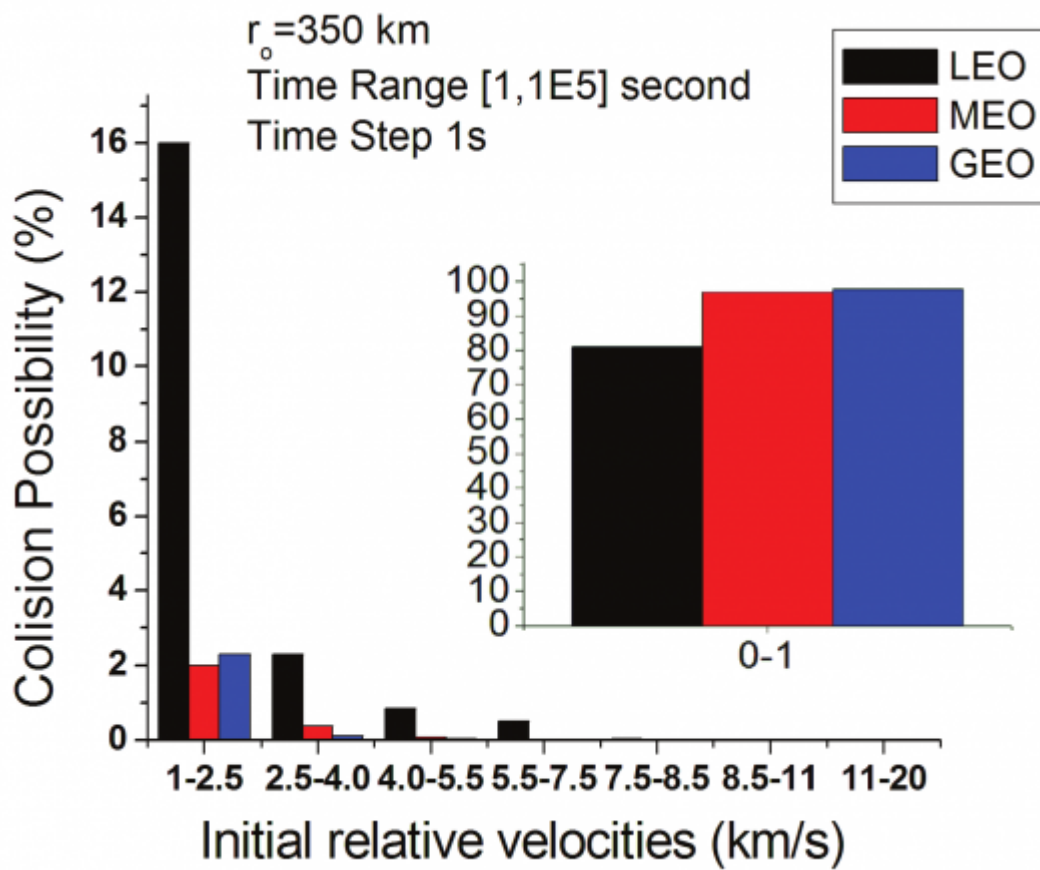


Figure 1:



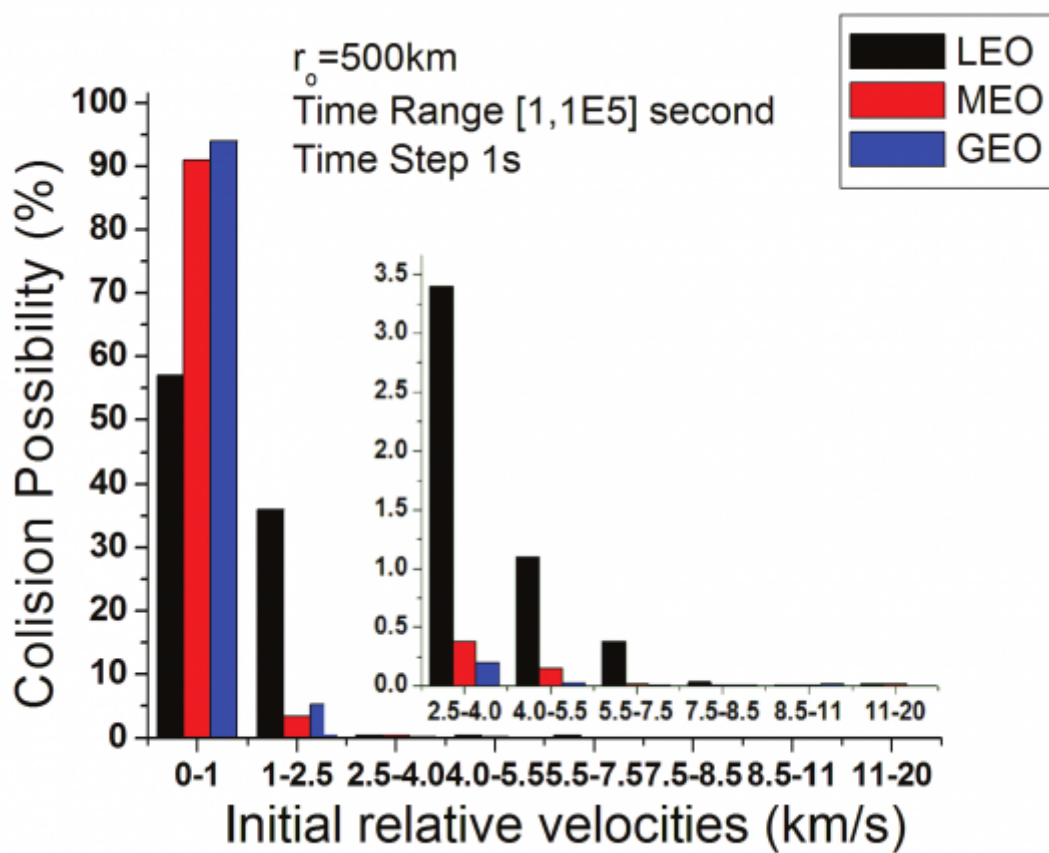
2

Figure 2: Figure 2 :



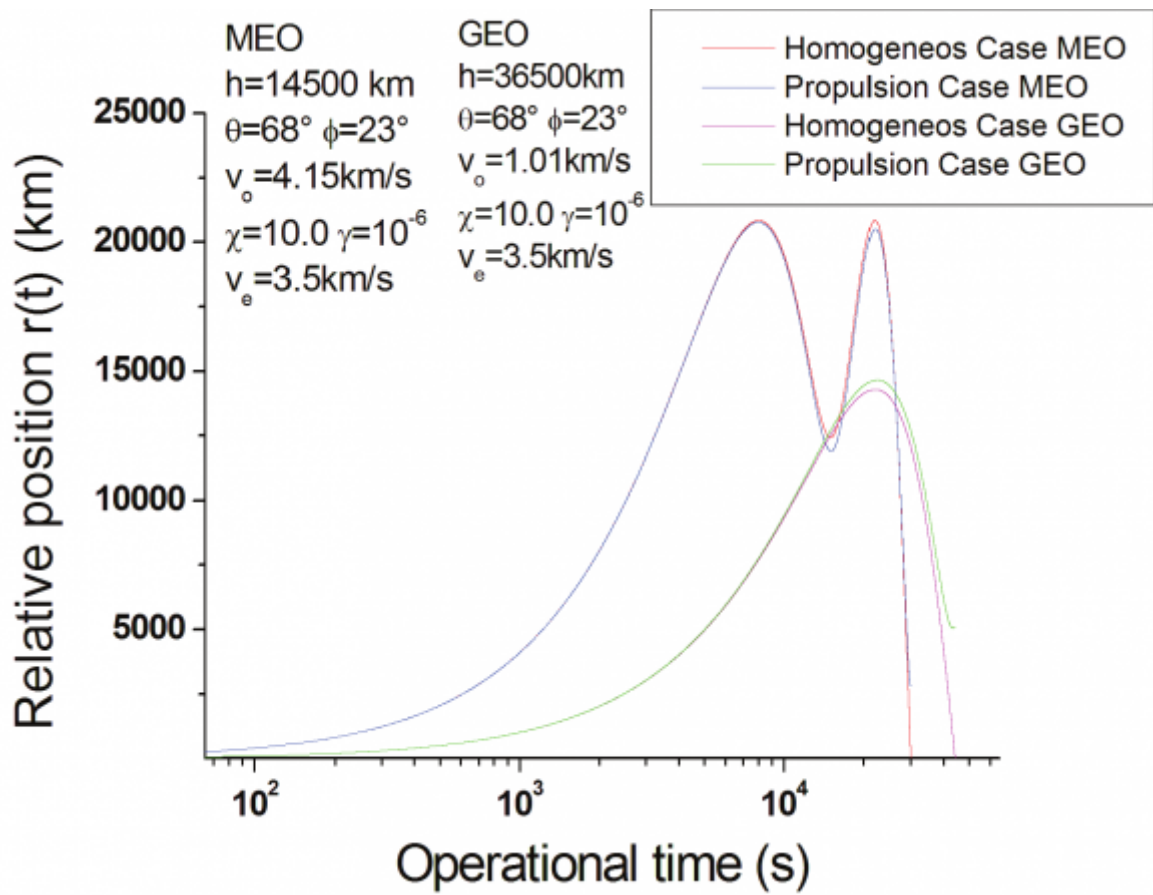
34

Figure 3: Figure 3 :Figure 4 :



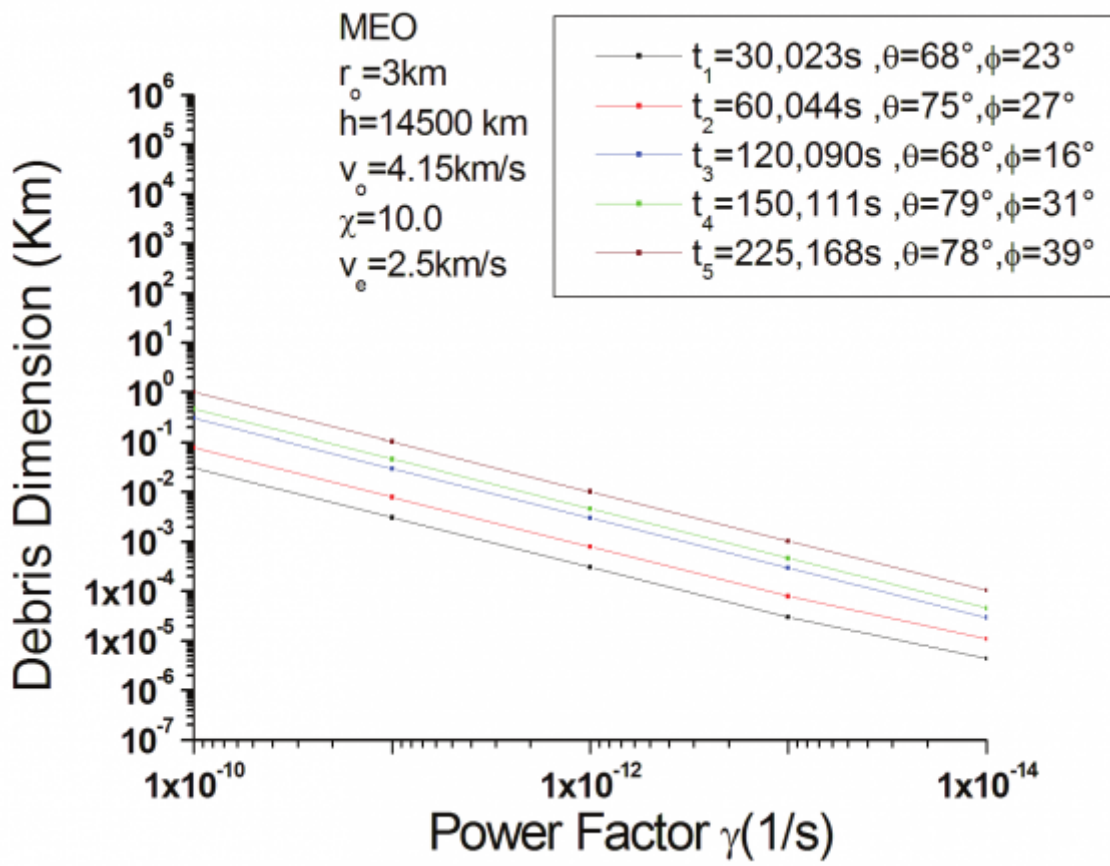
5

Figure 4: Figure 5 :



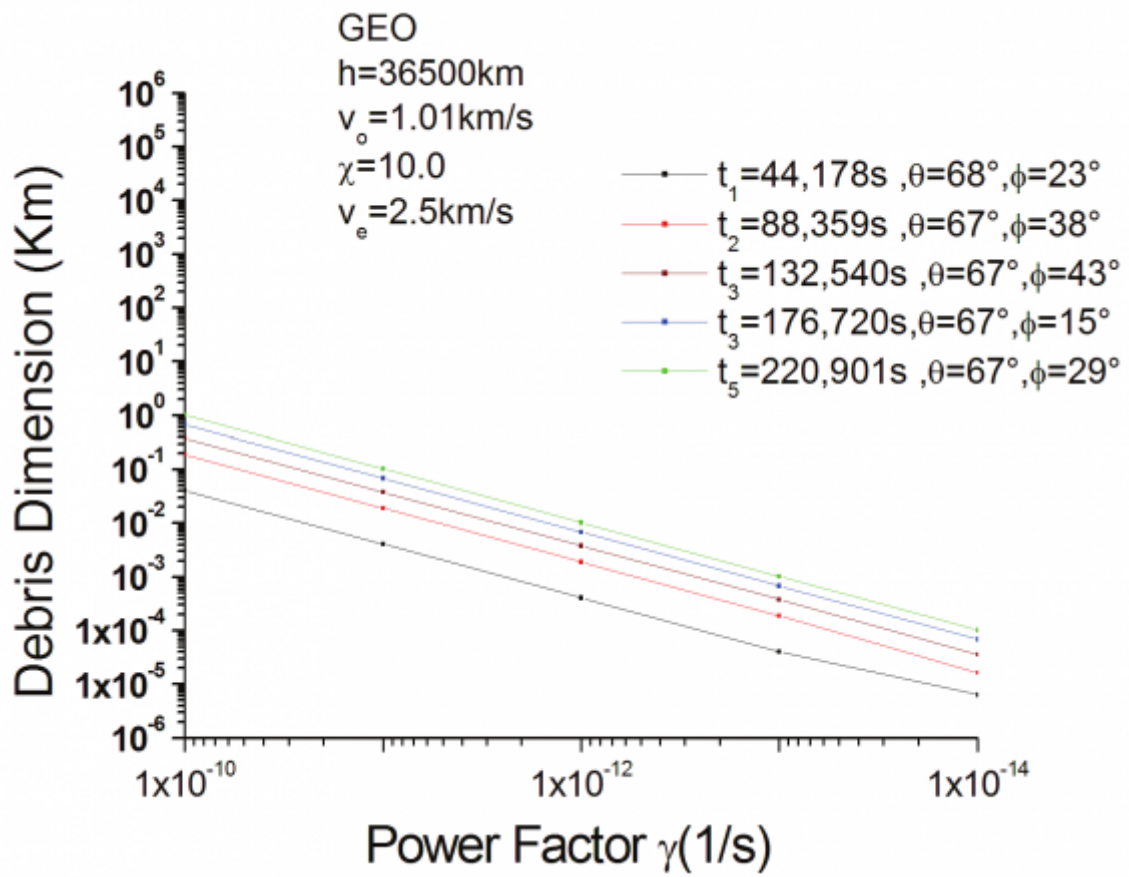
6

Figure 5: Figure 6 :



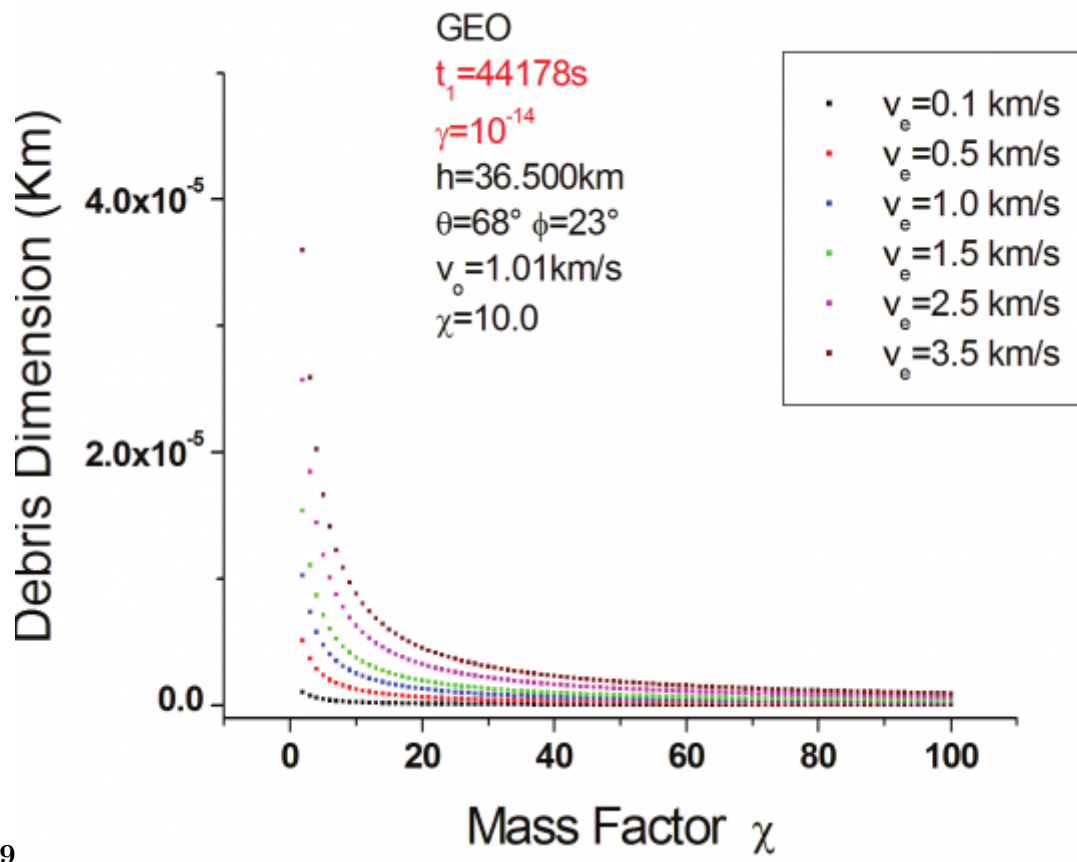
7

Figure 6: Figure 7 :



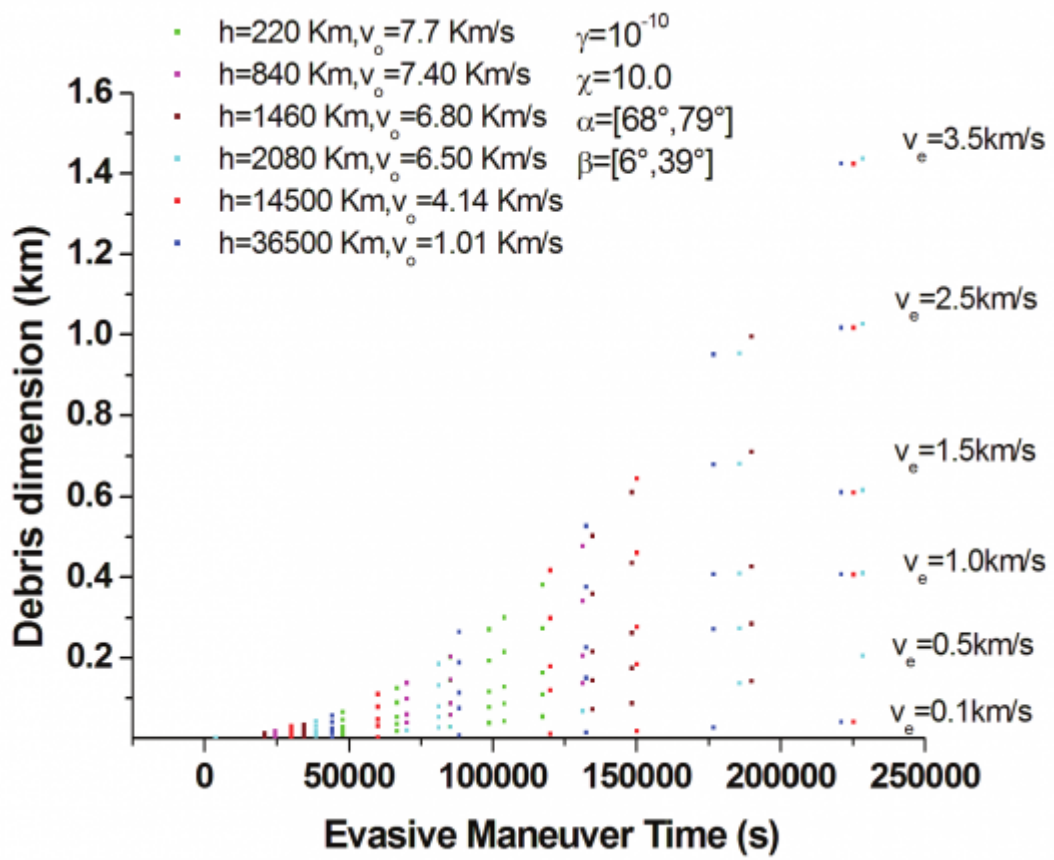
8

Figure 7: Figure 8 :



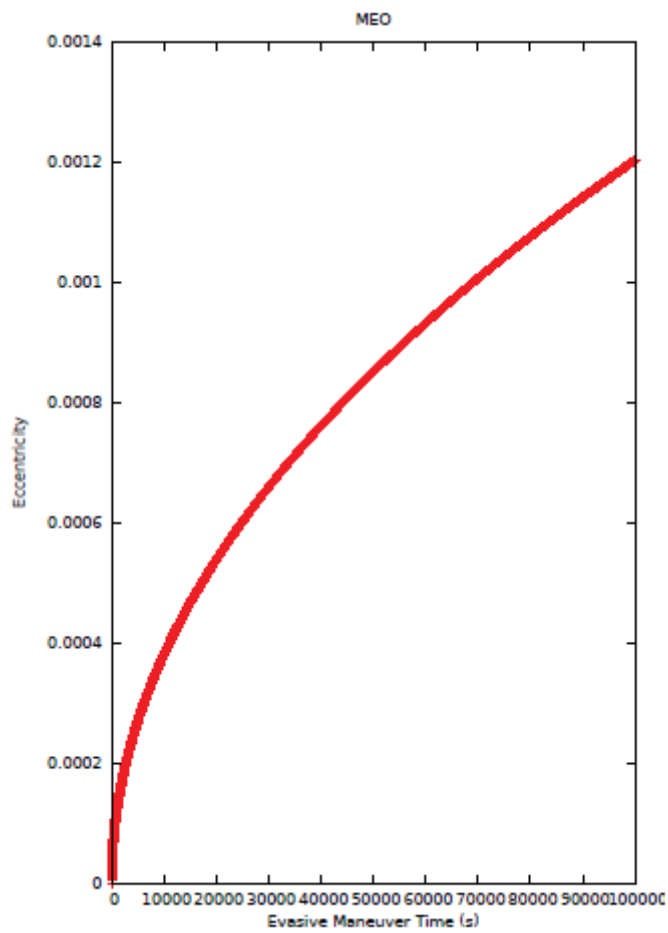
9

Figure 8: Figure 9 :



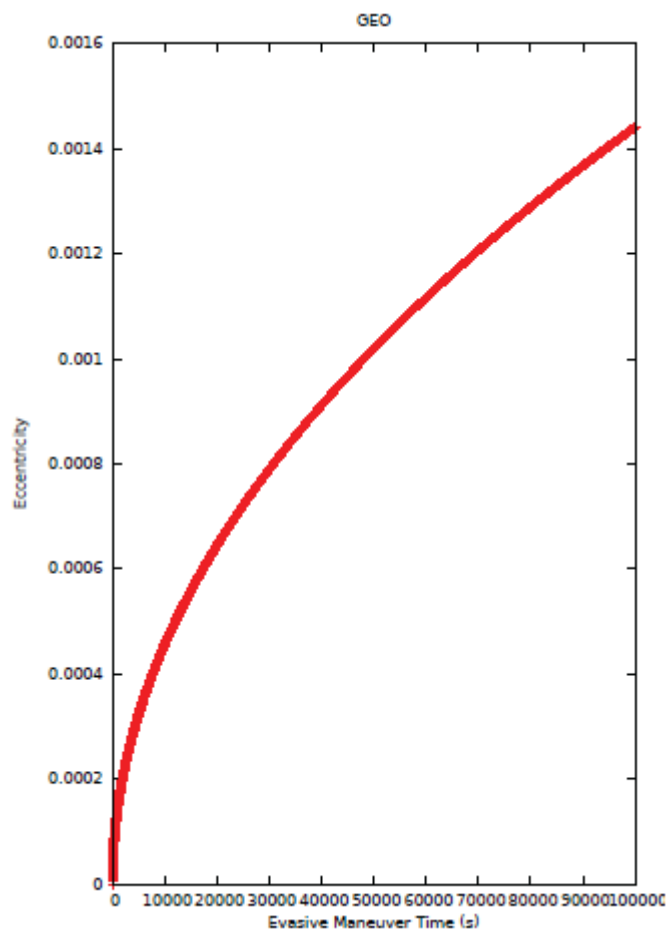
10

Figure 9: Figure 10 :



11A

Figure 10: Figure 11A :



12A

Figure 11: Figure 12A :

311 .1 Appendix A. Satellite Eccentricity Variation

312 The satellite eccentricity (e) can be written as a function of specific energy (ϵ) of its circular orbit by the equation
313 (Burns, 1976):

314 Where h is the angular momentum of the satellite orbit by mass unit, and μ is the product of the Earth's
315 mass by the gravitational universal constant. The satellite equation of motion with the gravitational force of the
316 Earth and the propulsion system is:

317 The propulsion accelerations are:

318 The power due to thrust produces variation in specific energy-orbit: is the velocity of satellite in the its circular
319 orbit.

320 The variation in the angular momentum is originated due to the applied torque is given by: The integration
321 of the equations above show us how the energy and the angular momentum of the satellite are modified by
322 the force of propulsion, these functions are respectively: Returned to equation (A.1) the time rate of change of
323 eccentricity the satellite orbit is due to variation in the angular momentum and energy of its orbit. Therefore, we
324 can calculate a function for the change in eccentricity in time: $\dot{e} = \frac{1}{R} \frac{d}{dt} (e R) = \frac{1}{2} \frac{d}{dt} (e^2 R)$ are specific energy and
325 the angular moment of satellite. The following shows the variation in the eccentricity of the satellite in function
326 of time avoidance maneuver for the two orbital regions MEO and GEO.

327 [Esa ()] , Esa . 2009.

328 [Esa ()] , Esa . 2013.

329 [Kessler and Cour-Palais ()] 'Collision frequency of artificial satellites: The creation of a debris belt'. D J Kessler
330 , B G Cour-Palais . *Journal of Geophysical Research: Space Physics* 1978. 1978-2012. 83 (A6) p. .

331 [Rossi and Valsecchi ()] 'Collision risk against space debris in earth orbits'. A Rossi , G Valsecchi . *Celestial
332 Mechanics and Dynamical Astronomy* 2006. 95 (1-4) p. .

333 [Kessler ()] 'Collisional cascading: The limits of population growth in low earth orbit'. D J Kessler . *Advances
334 in Space Research* 1991. 11 (12) p. .

335 [Godwin ()] *Columbia accident investigation report*, R Godwin . 2003. Burlington, Ont: Apogee Books. 39.

336 [Burns ()] 'Elementary derivation of the perturbation equations of celestial mechanics'. J A Burns . *American
337 Journal of Physics* 1976. 44 (10) p. .

338 [Johnson et al. ()] N L Johnson , J Gabbard , G Devere , Johnson , E . *13 history of on-orbit satellite
339 fragmentations*, 2004.

340 [Rossi et al. ()] 'Modelling the evolution of the space debris population'. A Rossi , L Anselmo , A Cordelli , P
341 Farinella , C Pardini . *Planetary and Space Science* 1998. 46 (11) p. .

342 [Milani et al. ()] *Nongravitational perturbations and satellite geodesy*, A Milani , A Nobill , P Farinella . 1987.

343 [Valk et al. ()] 'Semianalytical theory of mean orbital motion for geosynchronous space debris under gravitational
344 influence'. S Valk , A Lemaitre , F Deleflie . *Advances in Space Research* 2009. 43 (7) p. .

345 [Anselmo and Trumphy ()] 'Short-term predictions of cosmos 1402 reentry'. L Anselmo , S Trumphy . *Journal of
346 the Astronautical Sciences* 1986. 34 p. .

347 [Smirnov ()] *Space Debris: Hazard Evaluation and Debris*, N N Smirnov . 2001. CRC Press.

348 [Klinkrad ()] *Space Debris: Models and Risk Analysis*, H Klinkrad . 2006. Springer Science & Business Media.

349 [Rossi ()] 'The earth orbiting space debris'. A Rossi . *Serbian Astronomical Journal* 2005. 170 p. .

350 [Bendisich et al. ()] 'The master-2001 model'. J Bendisich , K Bunte , H Klinkrad , H Krag , C Martin , H Sdunnus
351 , R Walker , P Wegener , C Wiedemann . *Advances in Space Research* 2004. 34 (5) p. .